Matter

CellPress

Article

High-throughput experiments for rare-event rupture of materials

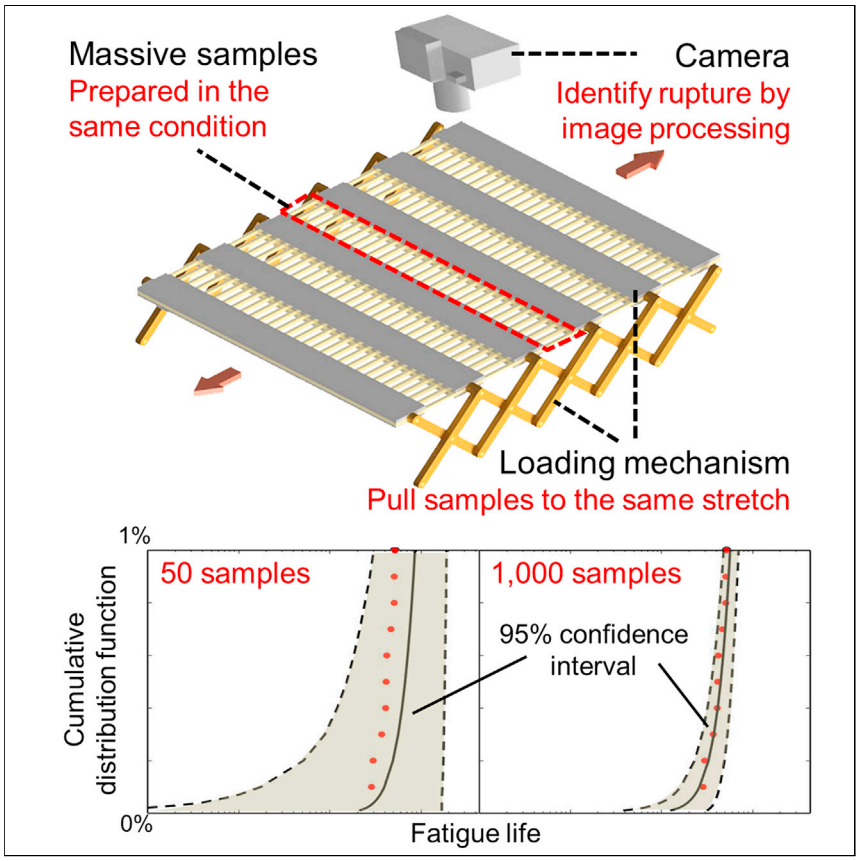

We develop a high-throughput experiment to study rare-event rupture. In a high-throughput experiment, we fabricate 1,000 samples, stretch them simultaneously, and identify rupture of individual samples. The data are analyzed statistically. The high-throughput experiment increases efficiency and enables the prediction of rare events.

Yifan Zhou, Xuhui Zhang, Meng Yang, ..., Jose Blanchet, Zhigang Suo, Tongqing Lu

jose.blanchet@gmail.com (J.B.)
suo@seas.harvard.edu (Z.S.)
tongqinglu@mail.xjtu.edu.cn (T.L.)

Highlights

Develop a high-throughput experiment to study rare-event rupture

Fabricate 1,000 samples and stretch them simultaneously

Identify rupture of individual samples by image processing

Analyze the data from the high-throughput experiment by extreme value statistics

6 **Development**
Practical, real world, technological considerations and constraints

Zhou et al., Matter 5, 1–12
February 2, 2022
https://doi.org/10.1016/j.matt.2021.12.017

Please cite this article in press as: Zhou et al., High-throughput experiments for rare-event rupture of materials, Matter (2021), https://doi.org/10.1016/j.matt.2021.12.017

Matter

CellPress

Article

High-throughput experiments for rare-event rupture of materials

Yifan Zhou,[1,4] Xuhui Zhang,[2,4] Meng Yang,[1] Yudong Pan,[1] Zhenjiang Du,[1] Jose Blanchet,[2,*] Zhigang Suo,[3,*] and Tongqing Lu[1,5,*]

SUMMARY

The conditions for rupture of a material commonly vary from sample to sample. Of great importance to applications are the conditions for rare-event rupture, but their measurements require many samples and consume much time. Here, the conditions for rare-event rupture are measured by developing a high-throughput experiment. For each run of the experiment, 1,000 samples are printed under the same nominal conditions and pulled simultaneously to the same stretch. Identifying the rupture of individual samples is automated by processing the video of the experiment. Under monotonic load, the rupture stretch for each sample is recorded. Under cyclic load, the number of cycles to rupture for each sample is also recorded. Rare-event rupture is studied by using the Weibull distribution and the peak-over-threshold method. This work reaffirms that predicting rare events requires large datasets. The high-throughput experiments enable the prediction of rare events with high accuracy and confidence.

INTRODUCTION

Predicting rupture of materials is of paramount importance. Rupture is a complex process taking place over many time and length scales. Despite decades of intense efforts, theory and computation alone can seldom predict the conditions for rupture.[1–5] Rather, the common practice is to measure the conditions for rupture by experiments.[6,7] For a given material, the measured conditions for rupture commonly scatter widely from sample to sample. For example, when a brittle solid (e.g., a ceramic or a glass) is subjected to a monotonic load, the magnitude of stress to rupture scatters from multiple GPa to multiple MPa.[8,9] As another example, when a ductile solid (e.g., a metal or a plastic) is subjected to cyclic load of prescribed amplitude, the number of cycles to rupture scatters by orders of magnitude.[10,11] Consequently, conditions for low-probability rupture deviate greatly from those of the mean.[12] It is, however, the conditions of low-probability rupture that surprise the public and command the attention of the engineer. To observe rare-event rupture, the engineer must test a large number of samples under the same conditions. Observing rare events is extremely time consuming. A potential solution is to conduct high-throughput experiments.[13] This solution poses challenges in developing methods to fabricate and test a large number of samples.

Here, we develop a high-throughput experiment to study rare-event rupture of materials (Figure 1). We print 1,000 samples under the same nominal conditions. We program the printer to print the samples in five layers, along with six connective bars. We design a kinematic mechanism of one degree of freedom to deform all

Progress and potential

Engineers place a high premium on unexpected rupture of a material subjected to a small stretch or a small number of cycles. Under such conditions, rupture is a rare event. Predicting such a rare event requires tests of many samples and is extremely time-consuming. This paper describes a high-throughput experiment to obtain large datasets for the conditions of rupture. We load 1,000 samples of a material simultaneously, either monotonically or cyclically, and identify the rupture of individual samples by processing images automatically to detect ruptures. We analyze the data using extreme-value statistics. It is hoped that this work will motivate further the development of high-throughput experiments to predict rare events.

Please cite this article in press as: Zhou et al., High-throughput experiments for rare-event rupture of materials, Matter (2021), https://doi.org/10.1016/j.matt.2021.12.017

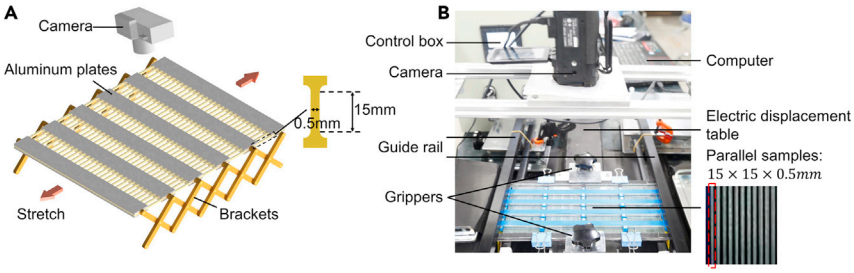

Figure 1. Experimental method

(A) A kinematic mechanism of one degree of freedom pulls a large number of samples simultaneously to the same stretch while a video camera records the experiment. Each sample has the shape of a dog bone.

(B) A photo of the experimental setup.

the samples by the same amount simultaneously. The length of a deformed sample divided by that of the undeformed sample defines the stretch λ. For such a large number of samples, it is impractical to identify the rupture of individual samples by the human eye. We record the video of each run of the experiment and write software that processes the video to identify rupture of individual samples. We conduct four runs of the experiment under monotonic load to a stretch of $\lambda = 2.2$, observe that 3,596 out of 4,000 samples rupture, and we record the rupture stretch of each sample. We also run the experiment under cyclic load to four amplitudes of stretch $\lambda =$ 1.6, 1.7, 1.8, and 1.9, observe that 3,996 samples rupture, and record the number of cycles to rupture of each individual sample. The large datasets enable us to analyze rare-event rupture by using the Weibull distribution and peak-over-threshold method from extreme-value statistics.

High-throughput experiments have long been developed. Such an experiment must resolve two main challenges: fabricate a large number of samples, and test them. Massive sample preparation is often achieved using methods such as printing and photolithography.[14–19] High-throughput experiments have been developed extensively to measure chemical, thermal, electrical, and biological properties,[20–24] but seldom to measure mechanical properties. To measure mechanical properties, one has to deform and rupture samples. Few such efforts have been reported. For example, the moduli and hardnesses of over 1,700 printed materials were measured one by one using nanoindentation; the measurements took about 24 h.[25] The strengths of 25 samples of printed stainless steel alloy were measured one by one using an automated tensile machine within 1 h[26] Such sequential methods are unsuitable for processes that take a long time. Examples of prolonged processes include rupture under cyclic load, creep, and slow crack growth. The time of tests can be reduced by loading many samples simultaneously. For example, in 1930, Cooper studied fatigue rupture of a rubber by cyclically loading eight samples simultaneously.[27] In a previous paper, we studied fatigue rupture of a hydrogel by cyclically loading six samples simultaneously.[28] Sun et al. studied delamination and cracking of many microfabricated inorganic islands on a plastic substrate.[18]

RESULTS AND DISCUSSION

We first stretch 1,000 samples monotonically (Video S1), setting the stretch rate as 0.15/min. In each run of the experiment, we stretch 1,000 samples from $\lambda = 1$ to $\lambda = 2.2$ and record the number of ruptured samples as a function of λ. The experiment is repeated four times. A representative experiment is illustrated with three snapshots. In the unstretched state, $\lambda = 1$, the 1,000 samples are intact (Figure 2A).

[1]State Key Laboratory for Strength and Vibration of Mechanical Structures, International Center for Applied Mechanics, Department of Engineering Mechanics, Xi'an Jiaotong University, Xi'an 710049, China

[2]Department of Management Science and Engineering, Stanford University, 475 Via Ortega, Stanford, CA 94305, USA

[3]John A. Paulson School of Engineering and Applied Science, Kavli Institute for Bionano Science and Technology, Harvard University, Cambridge, MA 02138, USA

[4]These authors contributed equally

[5]Lead contact

*Correspondence:
jose.blanchet@gmail.com (J.B.),
suo@seas.harvard.edu (Z.S.),
tongqinglu@mail.xjtu.edu.cn (T.L.)

https://doi.org/10.1016/j.matt.2021.12.017

Please cite this article in press as: Zhou et al., High-throughput experiments for rare-event rupture of materials, Matter (2021), https://doi.org/10.1016/j.matt.2021.12.017

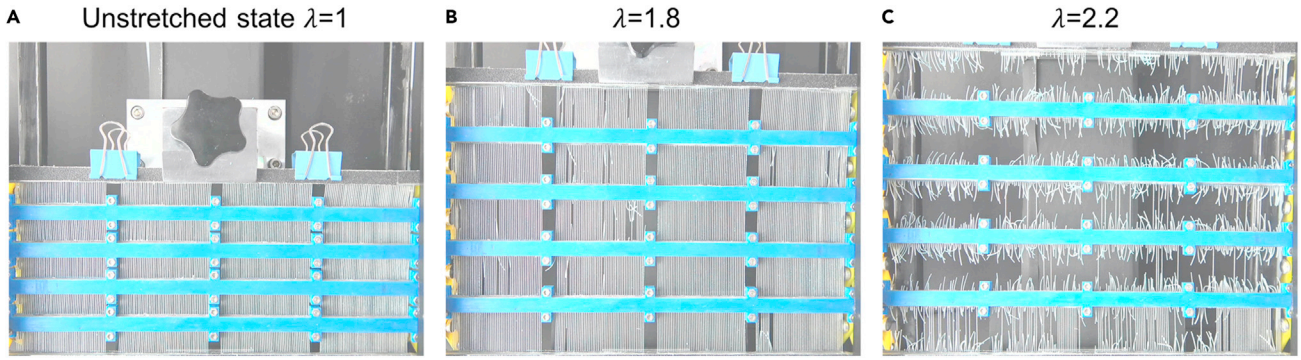

Figure 2. Rupture of samples under monotonic stretch
(A) A photo of 1,000 samples in the unstretched state.
(B) 34 samples have ruptured at stretch 1.8.
(C) 947 samples have ruptured at stretch 2.2.

At λ = 1.8, 34 samples have ruptured (Figure 2B). At λ = 2.2, 947 samples have ruptured (Figure 2C).

At a given stretch λ, let F be the number of ruptured samples divided by the total number of samples (1,000). We plot the cumulative distribution function (cdf), $F(\lambda)$, for each run of the experiment (Figure S1). The curves of four runs of the experiment nearly coincide, indicating that the experiment is statistically reproducible. We then aggregate the data of the four runs of the experiment. Of the 4,000 samples tested, a total of 3,596 samples rupture. Each ruptured sample corresponds to a data point in the $F-\lambda$ plane (Figure 3A). Following a common practice of statistics for rupture,[29] we fit the measured cdf to the three-parameter Weibull distribution:[30,31]

$$F(\lambda) = 1 - \exp\{-[(\lambda - \alpha)/\beta]^{\gamma}\} \qquad \text{(Equation 1)}$$

where α, β, and γ characterize the location, scale, and shape of the distribution. We determine the fitting parameters as α = 1.6709, β = 0.4175, and γ = 3.4404 using the maximum-likelihood Weibull fitting method.[32] The measured cdf approximately follows the Weibull distribution (solid curve) in the full range of data (Figure 3A). For a given value of the cumulative probability F, we further calculate the 95% confidence interval (CI) of the rupture stretch λ and plot in the F-λ plane as two dashed curves. The 95% CI appears to be narrow in the full range of data. However, the experimental data mostly lie outside the 95% CI. This indicates that the Weibull model is not appropriate to approximate the whole range of the cdf. To discuss rare-event rupture, we magnify the plots in Figure 3A in the range $0 \le F(\lambda) \le 1\%$ (Figure 3B). Similar to the overall fitting, in the range of rare events, a large portion of the experimental data, especially in the tail of interest, lies outside the 95% CI. That is, the Weibull fit using the data of all 4,000 tested samples is unable to predict the experimental data, including the rare events, with high confidence. The same conclusion is reached in an alternative way of evaluating the fitting results (Figure S2).

To achieve a prediction for rare-event rupture with accuracy and confidence, we adopt a procedure in the extreme-value statistics, called the peak-over-threshold method.[31] This method focuses on the statistics of the tail by imposing a threshold stretch. We apply the method to our data, and find the threshold stretch to be 1.87 (Figure S3). Of the 4,000 tested samples, 255 samples rupture at stretches below the threshold and are used to fit the Weibull distribution. With this method, all the experimental data in the range $0 \le F(\lambda) \le 1\%$ fall within the 95% CI (Figure 3C). For

Please cite this article in press as: Zhou et al., High-throughput experiments for rare-event rupture of materials, Matter (2021), https://doi.org/10.1016/j.matt.2021.12.017

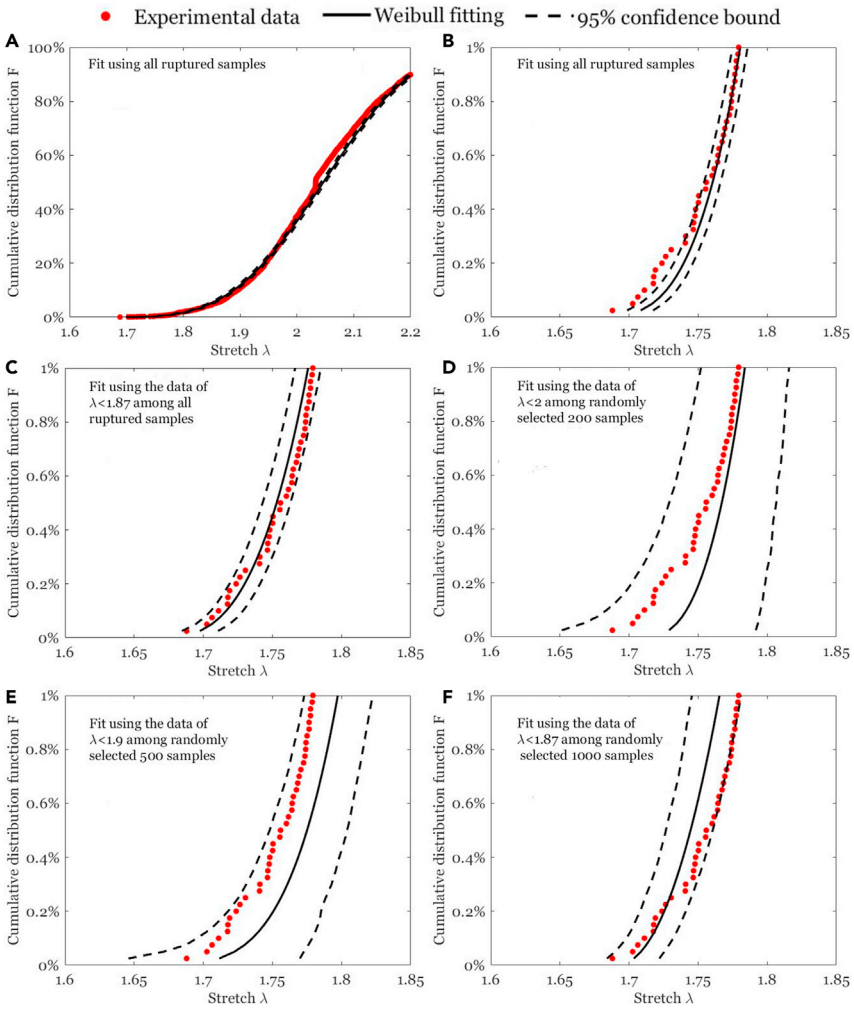

Figure 3. Probability of rupture under monotonic load

(A) The measured rupture stretches of 3,596 ruptured samples among 4,000 tested samples are used to calculate the cumulative distribution function (cdf), $F(\lambda)$. Each ruptured sample corresponds to a red dot in the F-λ plane. The measured cdf is fitted to the Weibull distribution (black solid line). Also plotted is the 95% CI (two black dashed lines).

(B) Blowup of the previous plots up to $F(\lambda) = 1\%$.

(C) The measured cdf up to the first 255 ruptured samples is fitted to the Weibull distribution. Also plotted are the 95% CI as well as the measured cdf of the first 40 ruptured samples.

(D) From the 4,000 tested samples, 200 samples are randomly selected. Of the 200 samples, 82 samples rupture at $\lambda < 2$. The cdf of these samples is fitted to the Weibull distribution and is used to calculate the 95% CI. Also included are the measured cdf of the first 40 ruptured samples among the 4,000 samples.

(E) 500 samples are randomly selected, and the data of $\lambda < 1.9$ are fitted to the Weibull distribution.

(F) 1,000 samples are randomly selected, and the data of $\lambda < 1.87$ are fitted to the Weibull distribution.

example, we specify a rare event by the cumulative probability $F(\lambda) = 0.1\%$, corresponding to the first four ruptured samples among the 4,000 tested samples. For the rare event of "0.1% rupture," the measured rupture stretch is $\lambda = 1.7111$, the Weibull fit is $\lambda = 1.7166$, and the 95% CI is $1.7056 < \lambda < 1.7288$. This high level of confidence as well as the narrow range of stretch are likely to satisfy most applications. By use of the peak-over-threshold method, the Weibull fit is reliable for prediction of rare-event rupture.

Please cite this article in press as: Zhou et al., High-throughput experiments for rare-event rupture of materials, Matter (2021), https://doi.org/10.1016/j.matt.2021.12.017

Normally, such a large dataset of rupture of testing 4,000 samples is unavailable, and the engineer needs to predict the rare-event rupture using whatever number of tested samples. To represent a smaller dataset, from the 4,000 tested samples we randomly select 200 samples. The peak-over-threshold method determines a threshold stretch $\lambda = 2$. Of the 200 samples, 82 samples rupture at stretches below the threshold and are used to fit the Weibull distribution and calculate the 95% CI (Figure 3D). Of the 200 samples, only one sample belongs to the range of $0 \leq F(\lambda) \leq 1\%$, and this sample falls within the 95% CI. However, the 95% interval is perhaps too wide to satisfy some engineers.

We next test the prediction of rare-event rupture by using the 200 samples. We plot the experimental data of all the 4,000 tested samples in the range of $0 \leq F(\lambda) \leq 1\%$. All the first 40 ruptured samples of the 4,000 samples fall within the 95% CI, even though only one of the 200 samples belongs to the range $0 \leq F(\lambda) \leq 1\%$. Thus, the dataset of the 200 samples can predict rare events with high confidence, but with a wide interval.

To narrow the 95% CI, datasets with more samples are needed. From the 4,000 tested samples we randomly select 500 and 1,000 samples, and repeat the statistical procedure (Figures 3E and 3F). As the number of selected samples increases, the 95% CI becomes narrower. The large dataset can predict rare events with both high confidence and narrow interval.

We next conduct high-throughput experiments of rupture under cyclic load (Video S2). The stretch rate is 0.2/s. In each run of the experiment, 1,000 samples are cycled between the undeformed state and a prescribed amplitude of stretch, λ. Such a test is conducted with four prescribed amplitudes of stretch, $\lambda = 1.6$, 1.7, 1.8, and 1.9. Each test is terminated when the number of cycles reaches 30,000. For each run of the experiment, snapshots are presented at four numbers of cycles (Figure 4). For example, for the test with the prescribed amplitude of stretch $\lambda = 1.6$, no sample ruptures after the first cycle, seven samples rupture after 500 cycles, 49 samples rupture after 1,000 cycles, and only four samples survive after 30,000 cycles. The number of cycles to rupture for individual samples, N, is obtained by processing the images from the recorded video.

We characterize the probability of fatigue rupture by the cdf, $F_\lambda(N)$, defined as the number of ruptured samples divided by the total number of samples at a given amplitude of stretch λ (Figure 5A). For each amplitude of stretch λ, we fit the cdf, $F_\lambda(N)$, to the three-parameter Weibull distribution function:

$$F_\lambda(N) = 1 - \exp\{-[(\ln(N) - \alpha)/\beta]^\gamma\} \qquad \text{(Equation 2)}$$

where α, β, γ are the location, scale, and shape parameters. The scatter in the number of cycles to rupture N is large. Following a common practice, we use $ln(N)$ instead of N in the Weibull distribution (Figure 5A). Using the maximum likelihood Weibull fitting method, we find that the parameters are $\alpha = 5.4835$, $\beta = 2.7763$, $\gamma = 3.7668$ for $\lambda = 1.6$; $\alpha = 3.4563$, $\beta = 3.6866$, $\gamma = 4.0735$ for $\lambda = 1.7$; $\alpha = 2.9149$, $\beta = 3.5968$, $\gamma = 4.6706$ for $\lambda = 1.8$; and $\alpha = 1.6939$, $\beta = 3.5867$, $\gamma = 6.4619$ for $\lambda = 1.9$. The measured cdf under cyclic loads approximately follows the Weibull distribution in the full range of the data, but a large portion of the data lies outside the 95% CI (Figure 5A). Figure 5B magnifies the plots in Figure 5A to show the cdf for $\lambda = 1.6$ up to $F_\lambda(N) = 1\%$. Similar to the fitting results under monotonic loads, using all the experimental data under cyclic loads, the Weibull fit is unable to predict fatigue

Please cite this article in press as: Zhou et al., High-throughput experiments for rare-event rupture of materials, Matter (2021), https://doi.org/10.1016/j.matt.2021.12.017

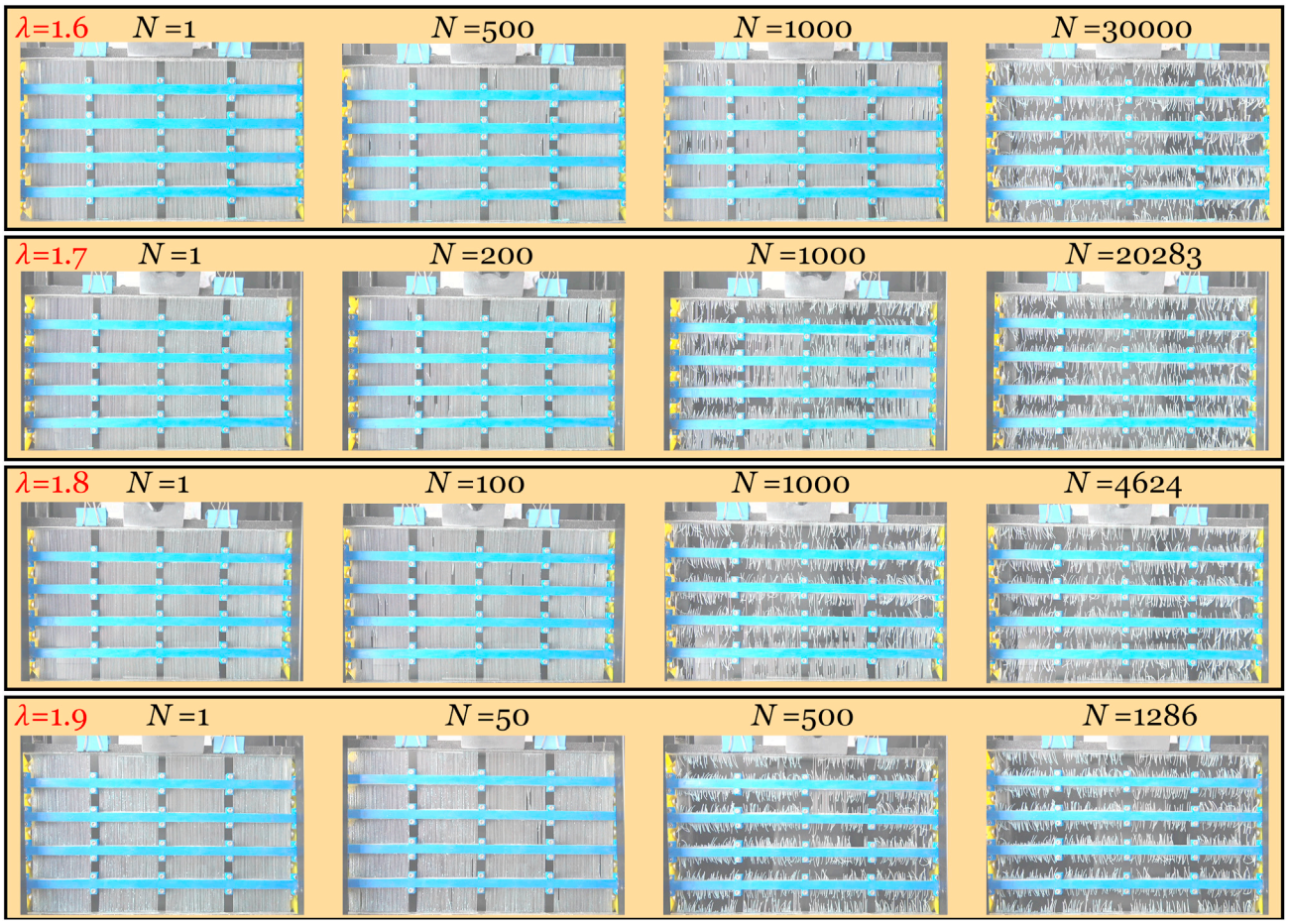

Figure 4. Rupture of samples under cyclic stretch

Samples are cyclically loaded to an amplitude of stretch, λ, to various numbers of cycles N. For each amplitude of stretch, λ, the test is terminated when the number of cycles reaches 30,000.

rupture with high confidence. We next use the data of the first 200 ruptured samples to fit the Weibull distribution and find that all the ruptured samples of the 1,000 tested samples fall within the 95% CI (Figure 5C). The large dataset gives a remarkably narrow interval of high confidence (Figure 5C). For example, for the rare event of "1% fatigue rupture," that is, the first 10 ruptured samples among the 1,000 tested samples, the measured number of cycles to rupture is $N = 517$, the Weibull fit is $N = 566$, and the 95% CI is $480 < N < 701$.

Obtaining a large dataset of fatigue rupture is much more time consuming than monotonic rupture. It is very often seen in the literature that only a few dozen samples are tested.[10] To mimic this common practice, we randomly select 50 samples from the 1,000 tested samples, and use the first 10 ruptured samples of the 50 samples to fit the Weibull distribution and calculate the 95% CI. To test the prediction of rare events, we plot the ruptured samples among all the 1,000 tested samples in the range of $0 \leq F(\lambda) \leq 1\%$. Selecting 50 samples from the 1,000 samples is random, so we repeat this procedure by selecting 50 samples from the 1,000 samples three times (Figures 5D–5F). The three fitting results show clear inconsistency: sometimes the experimental data fall outside the 95% CI (Figure 5E), and sometimes the 95% CI is very wide (Figure 5F). As far as the Weibull statistics is concerned, a small dataset is

Please cite this article in press as: Zhou et al., High-throughput experiments for rare-event rupture of materials, Matter (2021), https://doi.org/10.1016/j.matt.2021.12.017

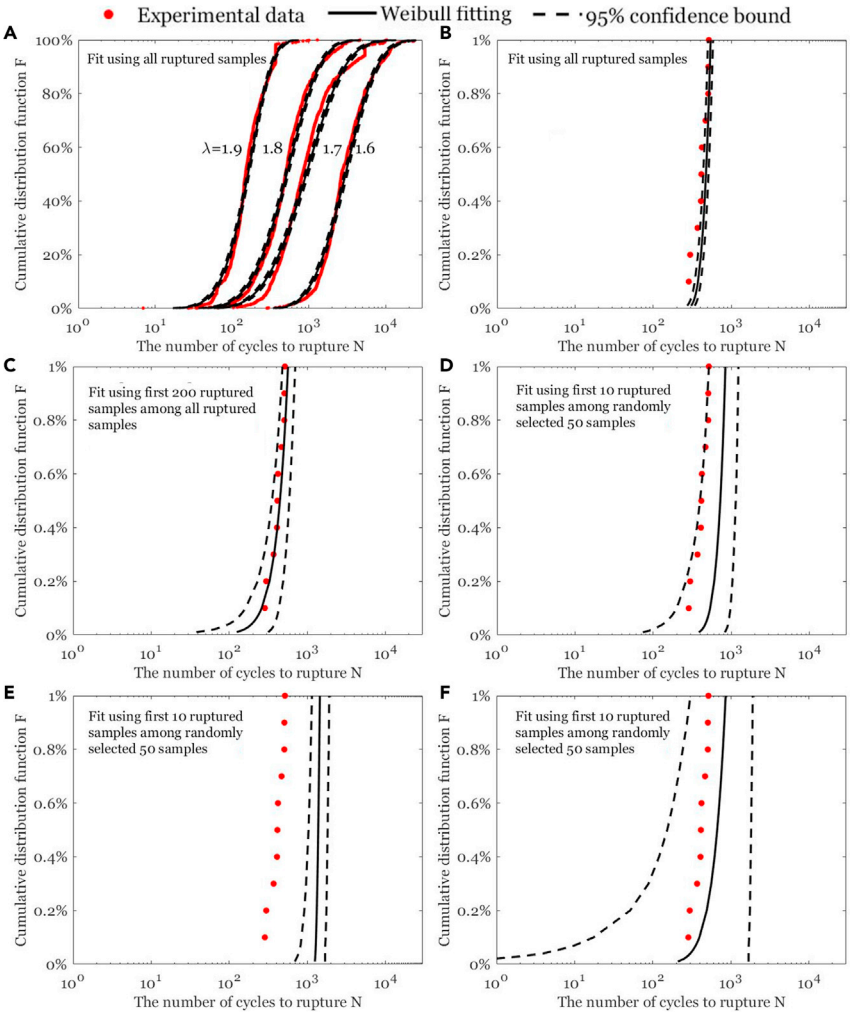

Figure 5. Probability of rupture under cyclic load

(A) The measured cdf $F_\lambda(N)$ is plotted as a function of N for several amplitudes of stretch λ. The data are fitted using the Weibull distribution and used to calculate the 95% CI.

(B) Blowup of the previous plots up to $F_\lambda(N) = 1\%$.

(C) The measured cdf of the first 200 ruptured samples are fitted to the Weibull distribution. Also plotted are the 95% CI, as well as the measured cdf of the first 10 ruptured samples.

(D–F) 50 samples are randomly selected, and the data of the first ruptured 10 samples are fitted to the Weibull distribution. The procedure is repeated three times.

unable to predict rare events with high confidence and narrow interval. Our experiments invalidate this common practice in the literature.

We also plot the prescribed amplitude of stretch, λ, against the number of cycles to rupture of each individual sample, N, in the $\lambda-N$ plane (Figure S4). This practice has been widely used to report fatigue data for small numbers of samples. For example, if each run of the test consists of only six samples, only six data points appear in the $\lambda-N$ plane.[28] These few data points visually display the mean and the scatter of fatigue life. However, when each run of the test has 1,000 samples, such a $\lambda-N$ plot becomes less meaningful (Figure S4). The large number of data points appear as a continuous line, which no longer visually displays the mean and the scatter of fatigue life.

Please cite this article in press as: Zhou et al., High-throughput experiments for rare-event rupture of materials, Matter (2021), https://doi.org/10.1016/j.matt.2021.12.017

In one run of the above experiments, either monotonic or cyclic, the distribution of ruptured samples may not be uniform. For example, more samples fail in the top and left parts in Figure 2C. Such nonuniformity makes testing 1,000 samples together in a high-throughput experiment different from testing 1,000 samples one by one in a conventional experiment. Both types of experiments introduce variations from sample to sample, but the causes for the variations can be different. The causes for variations in the high-throughput experiment deserve a careful study. The video of an experiment can be inspected by human eyes and analyzed by a combination of image processing and statistics to identify nonuniform distribution in ruptured samples. The identified nonuniformity can be used to pinpoint its cause. For example, the observation that more samples fail in the top and left parts suggests insufficient rigidity of the polymer brackets and aluminum plates. Other possible causes for nonuniformity include friction and vibration. Once identified, a cause for nonuniformity may be minimized by improving the experimental design. This iterative approach is fundamental to the design of the high-throughput experiment and will be reported in a subsequent work.

The current experiment uses 3D printed samples, but the high-throughput experiment can be modified to accommodate samples prepared by other methods, such as cutting and molding. Consider the case where a large piece of a material exists, such as a polyethylene film. The piece can be cut into a pattern of many dog-bone-shaped samples connected at their ends and then mounted simultaneously to the test frame. The high-throughput experiment can generate large datasets for fatigue of polyethylene. Next, consider the case where a large piece of a material does not exist, such as a type of biological tissue. A high-throughput experiment will require mounting individual samples to the test frame. The experiment will still save time in characterizing fatigue of the tissue. As noted before, multiple samples have long been tested simultaneously in fatigue experiments, although the number of samples has been small.[27] The method of image processing described here will allow such an experiment to be conducted for a large number of samples. The current high-throughput experiment is displacement controlled, whereas conventional mechanical tests sometimes are force controlled. We will report on force-controlled high-throughput experiments in a subsequent work.

Conclusions

In summary, we have developed a high-throughput experiment to study rare-event rupture of materials. We print a large number of samples under the same nominal conditions, design a kinematic mechanism of one degree of freedom to pull the samples simultaneously to the same stretch, and write software that analyzes the videos of the experiment to identify the rupture of individual samples. The large datasets are used to study the rare events of rupture at small stretches and small numbers of cycles. Our work reaffirms a truism: predicting the statistics of rare events with a narrow interval of high confidence requires large datasets. It is hoped that further studies will soon take place to advance high-throughput experiments and statistical methods to predict rare events.

EXPERIMENTAL PROCEDURES

Resource availability

Lead contact

Further information and requests for resources and reagents should be directed to and will be fulfilled by the lead contact, Tongqing Lu (tongqinglu@mail.xjtu.edu.cn).

Please cite this article in press as: Zhou et al., High-throughput experiments for rare-event rupture of materials, Matter (2021), https://doi.org/10.1016/j.matt.2021.12.017

Materials availability

The materials generated in this study are available from the corresponding author upon request.

Data and code availability

The data used to support the findings of this study are available from the corresponding author upon request.

Sample preparation

The 1,000 samples are evenly distributed in five layers (Figure 1). Each sample has a dumbbell shape, with the size of the central part being 15 × 0.5 × 0.5 mm. The five layers of samples are connected with six rectangular bars of dimension 300 × 10 × 0.5 mm. A 3D geometric description of the 1,000 samples and six rectangular bars is created in a CAD package, which is turned into .stl files for the Objet 350 printer (Connex3, Stratasys). The printer operates in the digital printing mode, with a resolution of height 30 μm. The 1,000 samples are printed with a mixture of three acrylic resins, Agilus30Clear, VeroYellow, and VeroCyan, with a weight proportion of 99.98%, 0.01% and 0.01%. The six rectangular bars are printed with VeroCyan. After the samples are printed, we use a spatula to gently remove the support material "support 706" from the samples, and use water to wash the samples. Minor damage is inevitable during the removal of the support material. We regard the random damage induced by removing the support material of each sample as an uncontrollable variable. This variable, together with other uncontrollable variables in the material preparation, causes the scatter in the conditions of rupture.

Experimental setup

The experimental setup includes a kinematic mechanism, an electric displacement table with a control box, a camera, and a computer (Figure 1B). The kinematic mechanism consists of diamond-shaped brackets connecting six aluminum plates. Each aluminum plate is bonded to a printed rectangular bar by using a cyanoacrylate glue. The two ends of the kinematic mechanism are fixed to two rigid grippers of the electric displacement table, which is powered and controlled by the control box. The connecting rods and the aluminum plates are connected through the screws, nuts, and bearings. Upon stretching, the samples elongate in the direction of stretch, the aluminum plates undergo rigid-body translation in the same direction, and the connecting rods rotate around the hinges. The kinematic mechanism moves with the two grippers with one degree of freedom and pulls all the 1,000 samples simultaneously to the same stretch. Guide rails are introduced to avoid rotation of the kinematic mechanism. The experiment is conducted in a black background and videotaped by a camera fixed above. The recorded video is transmitted to the computer by an acquisition card in real time.

Image processing

The recorded videos are processed using the software PotPlayer, which automatically outputs an image at a fixed time interval. The interval is 100 ms for the test under monotonic load and is 1 s for the test under cyclic load. Each image is then processed into a 1,920 × 1,080 matrix using MATLAB. Each element in the matrix represents the grayscale of a pixel. The samples are white and the background is black. The elements of the matrix are then binarized: 0 for a pixel of a grayscale nearly white, and 255 for a pixel of a grayscale nearly black. For each layer of samples, we sum over each column of the matrix. When a sample is unbroken, the sum is zero. When a sample is broken, the sum is a large number (Figure S5). See Supplemental information Appendix for the codes (Data S1).

Please cite this article in press as: Zhou et al., High-throughput experiments for rare-event rupture of materials, Matter (2021), https://doi.org/10.1016/j.matt.2021.12.017

Weibull distribution fitting

We use the software R-studio to fit the cdf of the measured rupture stretches under monotonic load to the Weibull distribution (Equation 1), and fit the cdf of the measured number of cycles to rupture under cyclic load to the Weibull distribution (Equation 2) (Data S2).

Maximum-likelihood Weibull fitting method

We use the maximum-likelihood estimation method to determine the parameters in Equation 1 and Equation 2. The likelihood function is defined by the Weibull density:

$$L_n\left(X_{(1)},\cdots X_{(n)}\right) = \prod_{i=1}^{n_r} f\left(X_{(i)}\right)\left[1-F(X_{\max})\right]^{n-n_r} \qquad \text{(Equation 3)}$$

where L_n is the likelihood function based on n iid observations, $X_{(i)}$ is the rupture stretch or the logarithm of the number of cycles to rupture for the i-th ruptured sample, X_{max} is the right-censoring limit, n_r is the total number of uncensored observations, and $f(X_{(i)})$ is the probability density function of Weibull distribution evaluated at $X_{(i)}$. We carry out the maximum-likelihood fitting with the default numerical-optimization method using the function "optim" in R-studio.

Peak-over-threshold method

To fit the Weibull distribution with the data near the rare event under monotonic load, we use the likelihood function informed by the Poisson point process model:

$$L_n\left(X_{(1)},\cdots X_{(n)}\right) \propto \left(1-F(X_{\max})\right)^n \cdot \prod_{i=1}^{n_r}(\gamma/\beta)\cdot\left(\left(X_{(i)}-\alpha\right)/\beta\right)^{\gamma-1} \qquad \text{(Equation 4)}$$

The "$\propto$" indicates a proportionality constant independent of the paramters. To select the threshold stretch X_{max} used in the Poisson point process modeling,[31] we plot the empirical mean residual life plots (Figure S3), defined as:

$$E = \frac{1}{n_u}\left(\sum_{i=1}^{n_u}\left(u-X_{(i)}\right) : u \le X_{\max}\right) \qquad \text{(Equation 5)}$$

where E is the empirical mean excess residual, u is any given threshold, n_u is the number of observations, which is smaller than u. We choose X_{max} so that for $u \le X_{max}$ the pairs (u,E) are approximately linear. We carry out the maximum-likelihood fitting using the function "fitpp" and the function "mrlplot" from the package "POT" in R-studio. Notice that the package "POT" is intended for the extreme-maxima modeling, whereas our interest is the modeling of the extreme minima. We therefore modify the stretch values to their negative values before passing the dataset into these functions to transform our original problem to an equivalent extreme-maxima modeling problem.

Estimated parameters and CI

After the above fitting procedures 3.4.1 and 3.4.2, we obtain both the fitted parameters $\widehat{\theta}$ and the observed Fisher information matrix $\mathcal{I}$.[31] The sampling distribution of the fitted parameters $\widehat{\theta}$ approximately obey the normal distribution $N(\theta,\mathcal{I}^{-1})$, where θ are the underlying true parameters (α, β, γ). We then construct the sampling distribution of the fitted stretches (as in the experiments with monotonic loads) or the number of cycles to rupture (as in the experiments with cyclic loads) by the inverse function of Equations 1 and 2. The CI is obtained by truncating the sample distribution. For example, to plot the 95% CI, the confidence limits are the lower and upper 2.5% quantiles of the sampling distribution.

SUPPLEMENTAL INFORMATION

Supplemental information can be found online at https://doi.org/10.1016/j.matt.2021.12.017.

ACKNOWLEDGMENTS

The work at Xian Jiaotong University is supported by NSFC (No.11922210). The work at Stanford and Harvard is supported by the Air Force Office of Scientific Research under award number FA9550-20-1-0397.

AUTHOR CONTRIBUTIONS

Y.Z. and X.Z. contributed equally to this work. Y.Z., X.Z., M.Y., Z.S., and T.L. designed the research; Y.Z., M.Y., Y.P., and Z.D. performed research; Y.Z., X.Z., J.B., Z.S., and T.L. wrote the paper.

DECLARATION OF INTERESTS

The authors declare no competing interests.

Received: July 20, 2021
Revised: November 12, 2021
Accepted: December 23, 2021
Published: January 20, 2022

REFERENCES

1. Creton, C., and Ciccotti, M. (2016). Fracture and adhesion of soft materials: a review. Rep. Prog. Phys. *79*, 046601. https://doi.org/10.1088/0034-4885/79/4/046601.

2. Li, W.D., Liaw, P.K., and Gao, Y.F. (2018). Fracture resistance of high entropy alloys: a review. Intermetallics *99*, 69–83. https://doi.org/10.1016/j.intermet.2018.05.013.

3. Rajabi, A., Ghazali, M.J., and Daud, A.R. (2015). Chemical composition, microstructure and sintering temperature modifications on mechanical properties of TiC-based cermet – a review. Mater. Des. *67*, 95–106. https://doi.org/10.1016/j.matdes.2014.10.081.

4. Domun, N., Hadavinia, H., Zhang, T., Sainsbury, T., Liaghat, G.H., and Vahid, S. (2015). Improving the fracture toughness and the strength of epoxy using nanomaterials–a review of the current status. Nanoscale *7*, 10294–10329. https://doi.org/10.1039/c5nr01354b.

5. Bai, R.B., Yang, J.W., and Suo, Z.G. (2019). Fatigue of hydrogels. Eur. J. Mech. *74*, 337–370. https://doi.org/10.1016/j.euromechsol.2018.12.001.

6. Griffith, A.A. (1921). The phenomena of rupture and flow in solids. Phil. Trans. R. Soc. A: Math. Phys. Eng. Sci. *221*, 163–198. https://doi.org/10.1098/rsta.1921.0006.

7. Schütz, W. (1996). A history of fatigue. Eng. Fract. Mech. *54*, 263–300. https://doi.org/10.1016/0013-7944(95)00178-6.

8. Proctor, B., Whitney, I., and Johnson, J. (1967). The strength of fused silica. Proc. R. Soc. Lond. Ser. A. Math. Phys. Sci. *297*, 534–557.

9. Kurkjian, C.R., Krause, J.T., and Matthewson, M.J. (1989). Strength and fatigue of silica optical fibers. J. Lightwave Technol. *7*, 1360–1370. https://doi.org/10.1109/50.50715.

10. Syzrantseva, K., and Syzrantsev, V. (2017). Determination of parameters of endurance limit distribution law of material by the methods of nonparametric statistics and kinetic theory of high-cycle fatigue. Key Eng. Mater. *736*, 52–57. https://doi.org/10.4028/www.scientific.net/KEM.736.52.

11. Kawai, M., and Yano, K. (2016). Anisomorphic constant fatigue life diagrams of constant probability of failure and prediction of P–S–N curves for unidirectional carbon/epoxy laminates. Int. J. Fatig. *83*, 323–334. https://doi.org/10.1016/j.ijfatigue.2015.11.005.

12. Ballarini, R., Pisano, G., and Royer-Carfagni, G. (2016). The lower bound for glass strength and its interpretation with generalized Weibull statistics for structural applications. J. Eng. Mech. *142*, 04016100. https://doi.org/10.1061/(asce)em.1943-7889.0001151.

13. Liu, Y.H., Hu, Z.H., Suo, Z.G., Hu, L.Z., Feng, L.Y., Gong, X.Q., Liu, Y., and Zhang, J.C. (2019). High-throughput experiments facilitate materials innovation: a review. Sci. China-Technol. Sci. *62*, 521–545. https://doi.org/10.1007/s11431-018-9369-9.

14. Burger, B., Maffettone, P.M., Gusev, V.V., Aitchison, C.M., Bai, Y., Wang, X., Li, X., Alston, B.M., Li, B., Clowes, R., et al. (2020). A mobile robotic chemist. Nature *583*, 237–241. https://doi.org/10.1038/s41586-020-2442-2.

15. Libonati, F., Gu, G.X., Qin, Z., Vergani, L., and Buehler, M.J. (2016). Bone-inspired materials by design: toughness amplification observed using 3D printing and testing. Adv. Eng. Mater. *18*, 1354–1363. https://doi.org/10.1002/adem.201600143.

16. Ngo, T.D., Kashani, A., Imbalzano, G., Nguyen, K.T.Q., and Hui, D. (2018). Additive manufacturing (3D printing): a review of materials, methods, applications and challenges. Compos. B Eng. *143*, 172–196. https://doi.org/10.1016/j.compositesb.2018.02.012.

17. Xiang Gu, G., Su, I., Sharma, S., Voros, J.L., Qin, Z., and Buehler, M.J. (2016). Three-dimensional-printing of bio-inspired composites. J. Biomech. Eng. *138*, 021006. https://doi.org/10.1115/1.4032423.

18. Sun, J.Y., Lu, N.S., Oh, K.H., Suo, Z.G., and Vlassak, J.J. (2013). Islands stretch test for measuring the interfacial fracture energy between a hard film and a soft substrate. J. Appl. Phys. *113*, 223702. https://doi.org/10.1063/1.4810763.

19. Seisyan, R.P. (2011). Nanolithography in microelectronics: a review. Tech. Phys. *56*, 1061–1073. https://doi.org/10.1134/S1063784211080214.

20. Green, M.L., Choi, C.L., Hattrick-Simpers, J.R., Joshi, A.M., Takeuchi, I., Barron, S.C., Campo, E., Chiang, T., Empedocles, S., Gregoire, J.M., et al. (2017). Fulfilling the promise of the materials genome initiative with high-throughput experimental methodologies. Appl. Phys. Rev. *4*, 011105. https://doi.org/10.1063/1.4977487.

21. Green, M.L., Takeuchi, I., and Hattrick-Simpers, J.R. (2013). Applications of high throughput (combinatorial) methodologies to electronic, magnetic, optical, and energy-related

materials. J. Appl. Phys. *113*, 231101. https://doi.org/10.1063/1.4803530.

22. Webster, D.C. (2008). Combinatorial and high-throughput methods in macromolecular materials research and development. Macromol. Chem. Phys. *209*, 237–246. https://doi.org/10.1002/macp.200700558.

23. Huang, J.X., Lee, G., Cavanaugh, K.E., Chang, J.W., Gardel, M.L., and Moellering, R.E. (2019). High throughput discovery of functional protein modifications by hotspot thermal profiling. Nat. Methods *16*, 894–901. https://doi.org/10.1038/s41592-019-0499-3.

24. Guo, M.T., Rotem, A., Heyman, J.A., and Weitz, D.A. (2012). Droplet microfluidics for high-throughput biological assays. Lab Chip *12*, 2146–2155. https://doi.org/10.1039/c2lc21147e.

25. Tweedie, C.A., Anderson, D.G., Langer, R., and Van Vliet, K.J. (2005). Combinatorial material mechanics: high-throughput polymer synthesis and nanomechanical screening. Adv. Mater. *17*, 2599. https://doi.org/10.1002/adma.200501142.

26. Heckman, N.M., Ivanoff, T.A., Roach, A.M., Jared, B.H., Tung, D.J., Brown-Shaklee, H.J., Huber, T., Saiz, D.J., Koepke, J.R., Rodelas, J.M., et al. (2020). Automated high-throughput tensile testing reveals stochastic process parameter sensitivity. Mater. Sci. Eng. a-Struct. Mater. Prop. Microst. Process. *772*, 138632. https://doi.org/10.1016/j.msea.2019.138632.

27. Cooper, L.V. (1930). Laboratory evaluation of flex-cracking resistance. Ind. Eng. Chem. *2*, 0391–0394. https://doi.org/10.1021/ac50072a018.

28. Zhou, Y., Hu, J., Zhao, P., Zhang, W., Suo, Z., and Lu, T. (2021). Flaw-sensitivity of a tough hydrogel under monotonic and cyclic loads. J. Mech. Phys. Sol. *153*, 104483. https://doi.org/10.1016/j.jmps.2021.104483.

29. Doremus, R.H. (1983). Fracture statistics - a comparison of the normal, Weibull, and Type-I extreme value distributions. J. Appl. Phys. *54*, 193–198. https://doi.org/10.1063/1.331731.

30. Weibull, W. (2013). Fatigue testing and analysis of results (Elsevier).

31. Coles, S. (2001). An introduction to statistical modeling of extreme values (Springer).

32. Millar, R.B. (2011). Maximum Likelihood Estimation and Inference: With Examples in R, SAS and ADMB (John Wiley & Sons).